J. Cent. South Univ. (2021) 28: 2285−2294
DOI: https://doi.org/10.1007/s11771-021-4769-8

Springer

Influence of temperature on creep behavior, mechanical properties and microstructural evolution of an Al-Cu-Li alloy during creep age forming

ZHOU Chang(周畅)[1], ZHAN Li-hua(湛利华)[1, 2, 3], LI He(李贺)[1],
ZHAO Xing(赵兴)[1, 2, 3], HUANG Ming-hui(黄明辉)[1, 2, 3]

1. College of Mechanical and Electrical Engineering, Central South University, Changsha 410083, China;
2. State Key Laboratory of High-Performance Complex Manufacturing, Central South University, Changsha 410083, China;
3. Light Alloys Research Institute, Central South University, Changsha 410083, China

Abstract: The effect of temperature in range of 155−175 °C on the creep behavior, microstructural evolution, and precipitation of an Al-Cu-Li alloy was experimentally investigated during creep ageing deformation under 180 MPa for 20 h. Increasing temperature resulted in a noteworthy change in creep ageing behaviour, including a variation in creep curves, an improvement in creep rate during early creep ageing, and an increased creep strain. Tensile tests indicate that the specimen aged at higher temperature reached peak strength within a shorter time. Transmission electron microscopy (TEM) was employed to explore the effect of temperature on the microstructural evolution of the AA2198 during creep ageing deformation. Many larger dislocations and even tangled dislocation structures were observed in the sample aged at higher temperature. The number of T_1 precipitates increased at higher ageing temperature at the same ageing time. Based on the analysed results, a new mechanism, considering the combined effects of the formation of larger dislocation structures induced by higher temperature and diffusion of solute atoms towards these larger or tangled dislocations, was proposed to explain the effect of temperature on microstructural evolution and creep behaviour.

Key words: Al-Cu-Li alloys; creep age forming; mechanical properties; microstructure; precipitation

Cite this article as: ZHOU Chang, ZHAN Li-hua, LI He, ZHAO Xing, HUANG Ming-hui. Influence of temperature on creep behavior, mechanical properties and microstructural evolution of an Al-Cu-Li alloy during creep age forming [J]. Journal of Central South University, 2021, 28(8): 2285−2294. DOI: https://doi.org/10.1007/s11771-021-4769-8.

1 Introduction

Creep age forming (CAF) is currently regarded as an efficient method to manufacture extra-large light weight and high performance panel products of aerospace metal structures by the combination of age hardening and creep deformation. The process keeps an external stress on the components at an ageing temperature for a certain time, and simultaneously obtains a sound material property [1−3]. To manufacture those large aluminum alloy components with promising mechanical properties using this CAF technology, it is important to study the effect of processing parameters on the creep ageing behaviour of the alloy, especially ageing temperatures.

Third generation aluminum-lithium (Al-Li) alloys, with a promising combination of properties such as a low density, high strength and toughness, excellent corrosion resistance, and high specific

Foundation item: Project(2017YFB0306300) supported by the National Key R&D Program of China; Projects(51601060, 51675538) supported by the National Natural Science Foundation of China
Received date: 2020-07-01; **Accepted date:** 2020-11-28
Corresponding author: ZHAN Li-hua, PhD, Professor; Tel: +86-13974874472; E-mail: yjs-cast@csu.edu.cn; ORCID: https://orcid.org/0000-0001-9419-4149

strength, have been of great interest to the aerospace applications [4, 5]. The ternary Al-Cu-Li system has been suggested to generate lots of precipitates in artificially aged tempers, mainly including GP zones, δ' (Al_3Li), β' (Al_3Zr), θ' (Al_2Cu), and T_1 (Al_2CuLi), and the most important precipitate is the T_1 phase [6, 7]. Extensive studies have reported that the T_1 phase forms as very thin semi-coherent hexagonal plates lying on a $\{111\}_{Al}$ habit plane. Compared with θ' phase forming as octagonal plates on the {100} planes, T_1 precipitates can produce a greater hardening effect owing to a particularly high aspect ratio [8−11]. These T_1 plates are very thin, about 1.3 nm, and their thickness is very stable with ageing time at temperatures within about 175 °C [12−14]. It has been widely shown that dislocations in matrix can act as heterogeneous nucleation sites for the T_1 precipitates, of which the mechanism involves prior segregation of Cu and Mg to dislocation lines especially in the regions where the dislocations are most curved [15−17]. As it is dislocation nucleated, introducing more dislocations into materials by pre-stretching can accelerate ageing kinetic, which attributes to an increase in the density of T_1 nucleation sites. The resultant finer T_1 phase distribution has been shown to decrease the average diffusion field size, so the matrix is depleted of solutes in a shorter timescale [9, 13].

Many prior researches have been carried out to explore the effects of temperatures on ageing behaviour of various heat-treated aluminum alloys. A proper temperature is considered as a key factor to achieve a satisfactory mechanical performance after artificially ageing. LYU et al [18] have investigated temperature dependence of stress relaxation ageing behaviour of an Al-Zn-Mg alloy and found that a high stress relaxation level with less than 15% strength loss can be obtained after 16 h forming below a suggested temperature of 165 °C. ZHANG et al [19] have reported that the constitution and morphology of precipitates within the AA2198 varies with ageing temperatures, and namely the major precipitates are δ', θ' when aged below 160 °C, while above 160 °C, T_1 phases in large number become dominate within the matrix. ZHU et al [20] have studied the effects of ageing temperatures on precipitation behaviour of a tensile deformed Al-Cu alloy, and concluded that with increasing temperature from 135 to 155 °C, the contents of θ'' phases and GP zones decrease, while that of θ' phases increases; if temperature is further raised, almost all the GP zones and θ'' phases will transform to θ' phases. ZOU et al [21] have showed that the work-hardenability of AA7085 at 90 °C is much better than that at 150 °C due to the predominance of GP II zones, and that the peak aged at 150 °C shows better corrosion resistance than that at 190 °C. ZHOU et al [22] have reported that the increase in ageing temperatures accelerates the progress of the entire creep, and both the creep strains and the room-temperature mechanical properties after creep ageing increase with the ageing temperature. However, there has been less published on the mechanism of the effect of temperature on creep ageing behaviour of an Al-Cu-Li alloy AA2198 alloy.

This study aims to examine the influence of ageing temperatures, ranging from 155 to 175 °C, on creep behaviour, microstructure, and T_1 precipitation of the AA2198. For this purpose, creep age testing and tensile tests were employed to determine the effect of temperature on the AA2198 alloy's creep ageing behaviour and mechanical performance after creep aged, respectively. TEM was utilized to observe the dislocation morphology and the evolution of the main strengthening phase, T_1. All data were used to discuss the mechanism of temperatures affecting on creep ageing behaviour of the AA2198.

2 Materials and methods

2.1 Materials and creep ageing testing procedures

AA2198 alloy, a typical third generation Al-Cu-Li alloy, was employed in this study. Plate with thickness of 2 mm, was supplied in a T3 temper. Table 1 lists the composition range of the AA2198 alloy. Creep ageing testing apparatus is shown in Figure 1(a). Specimens for creep ageing test in Figure 1(b) were spark machined along the rolling direction from the as-received plate. The applied stress usually was chosen to go below the yield strength of the initial material. The procedure was as follows: 1) The sample was heated to required ageing temperature at a rate of 5 °C/min, and then the specimen was loaded to the designated stress level of 180 MPa (lower than the yield strength of 237.6 MPa at T3 temper); 2) after reaching the set time, the creep aged specimen was removed from the furnace, and then air cooled to room temperature. The real-time temperature of the specimen was measured by a K-type thermocouple, tightly attaching to the specimen.

Table 1 Composition of AA2198 alloy (wt%)

Range	Cu	Li	Mg	Zr	Mn	Ag	Al
Min.	2.90	0.80	0.25	0.04	—	0.10	Bal.
Max.	3.50	1.10	0.80	0.18	0.50	0.50	Bal.

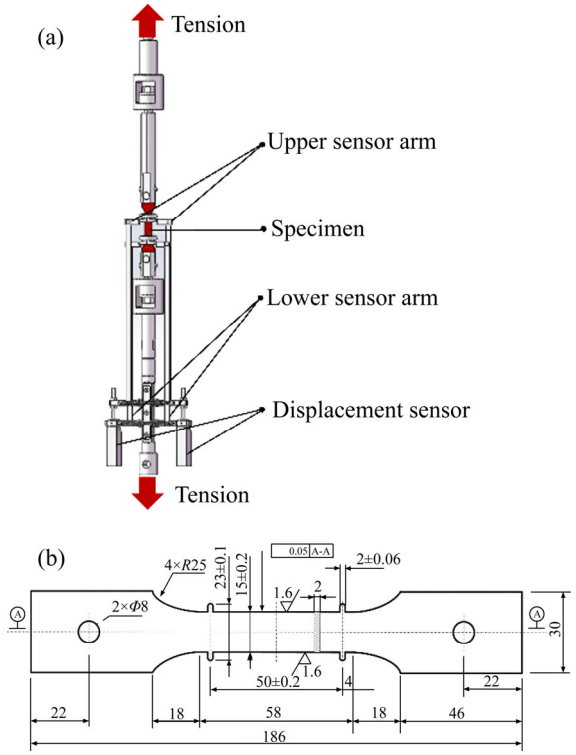

Figure 1 Schematic diagram of creep ageing apparatus (a) and geometry of specimen (Unit: mm) (b)

2.2 Tensile tests and microstructure characterization

Tensile testing was carried out using an MTS Alliance RT/100 tensile apparatus at a strain rate of 2 mm/min, with the strain monitored by a 50 mm clip gauge extensometer. Samples for TEM analysis were prepared by twin-jet electropolishing using a solution of 80% methanol and 20% nitric acid (volume fraction) at −20° under 15 V. TEM imaging was performed using a Tecnai G2 T20 microscope operating at 200 kV. Aberration-corrected scanning TEM (STEM) observation, which equipped with dual CEOS aberration correctors, was carried out using a FEI Titan 80-200 FEG-TEM.

3 Results and discussion

3.1 Effect of temperature on creep behaviour

Figure 2 shows the creep ageing curves of three specimens, respectively aged at 155, 165 and 175 °C under the applied stress level of 180 MPa for 20 h on AA2198 alloy. Corresponding creep strain rate curves are also plotted at different ageing temperatures, as shown in Figure 3. Typical two-stage creep behaviour consists of a primary creep stage where creep strain rate decreases quickly and a steady state secondary creep stage with a relatively stable creep rate. The specimen aged at 155 °C demonstrates a special creep behaviour, which is distinct from the conventional two-stage creep behaviour, both two particular stages with creep rate of zero (II-stage) and another with an increasing creep rate (III-stage), are observed during the whole creep ageing test. This creep ageing curve of the specimen aged at 155 °C can be divided into four stages based on the creep strain rate evolution, i.e., decreasing, being zero, increasing, and relatively stable creep strain rate in Figure 3. This special four-stage creep ageing behaviour can be described as the "multi-stage creep feature", as presented in Figure 2(b). Noted that Stage II of creep ageing behaviour was observed to have decreasing duration as a function of the increasing temperatures during the creep ageing tests, especially the disappearance

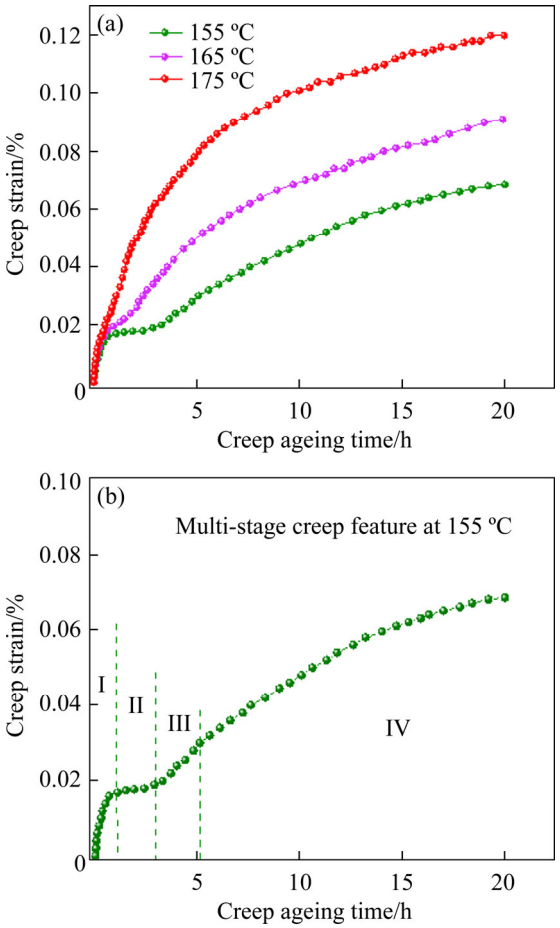

Figure 2 Creep curves at different ageing temperatures under 180 MPa for 20 h (a) and "multi-stage creep feature" for AA2198 at 155 °C (b)

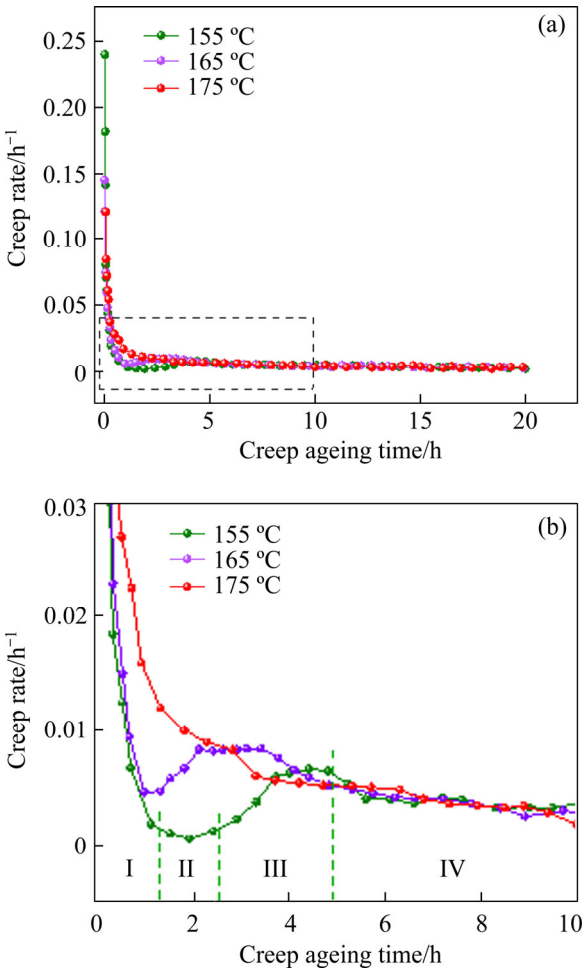

Figure 3 Corresponding creep strain rate curves under stress of 180 MPa for 20 h, with elevating ageing temperatures of 155, 165 and 175 °C (a) and enlarged view of the rectangular region(b)

of Stage II happening at 175 °C. The specimen aged at 175 °C exhibits the conventional two-stage creep behaviour (seen in Figure 3), which comprises of a primary creep stage where creep strain rate decreases quickly and a steady-state secondary creep stage with a relatively stable creep strain rate. Namely, both Stage II and Stage III seen in the 155 and 165 °C creep ageing tests were observed to disappear owing to the effects of higher temperature, which would lead to an increase in creep deformation efficiency. On the other hand, an increase in creep strains induced by higher temperatures was clearly observed, especially happening at the early creep ageing stage of about 5 h.

3.2 Effect of temperature on mechanical properties

Figure 4 shows the comparison of the evolution of average mechanical properties (from 3 tests), including yield stress, tensile strength, and elongation (plastic strain to failure), obtained from tensile testing specimens of creep ageing at various ageing temperatures. Although, similar evolution trends of strength and ductility along creep ageing time was observed from the whole age-strengthening curves for the creep aged specimens at different

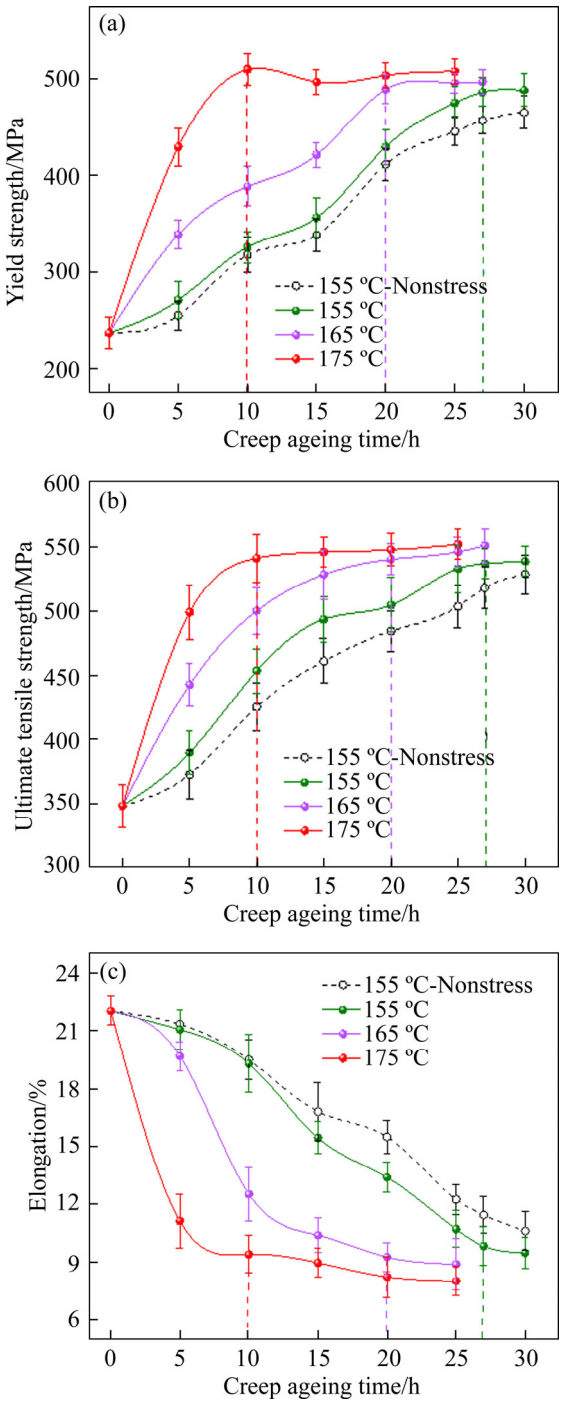

Figure 4 Evolution of mechanical as a function of creep ageing time for specimens aged at 155, 165 and 175 °C under stress of 180 MPa: (a) Yield stress; (b) Tensile strength; (c) Elongation

temperatures, the strength of specimen aged at higher temperatures was obviously higher than that of the aged at 155 °C and the corresponding elongation of the aged at higher temperatures was lower for the same creep ageing times. With time increasing to the peak-aged status, the peak strength and elongation at 155, 165 and 175 °C were almost the same. Besides, it can also be observed that the specimen aged at 175 °C experiences a shorter time by 17 h to obtain the peak strength, compared to that of specimen aged at 155 °C. These results indicate an acceleration in evolution of strength by higher ageing temperatures.

3.3 Effect of temperature on microstructure

3.3.1 Dislocation morphology

TEM imaging was employed to observe the dislocation evolution of the samples aged at different temperatures, focusing on the dislocation density and structures. Dislocations in the *T*3 initial temper of the AA2198 alloy exhibit a minior density and inhomogneously distribut within the matrix, as shown in Figure 5. Upon creep ageing at 155 °C for 1 h, the slightly higher dislocation density (seen in Figure 6(a)) introduced by creep deformation at applied stress of 180 MPa was observed to present throughout the aluminum matrix. With raising temperature to 165 °C, an obvious increase in dislocation density was observed comparing to that subjected to 155 °C for 1 h, and small and dense dislocation lines distributed within the matrix. Surprisingly, samples subjected to higher temperature of 175 °C show the presence of a higher density of dislocations, compared to that of the sample aged at 165 °C. Moreover, it was observed that dislocation lines grow to larger structures at higher temperatures, in the form of dense tangled forest (seen in Figure 6(c)). The above observed results can confirm that an apparent increase in the dislocation density and an obvious evolution in dislocation structures take place at higher ageing temperatures.

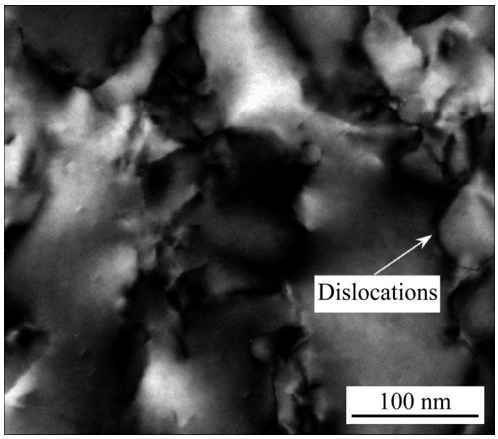

Figure 5 Bright field TEM image showing dislocations of sample in T3 temper

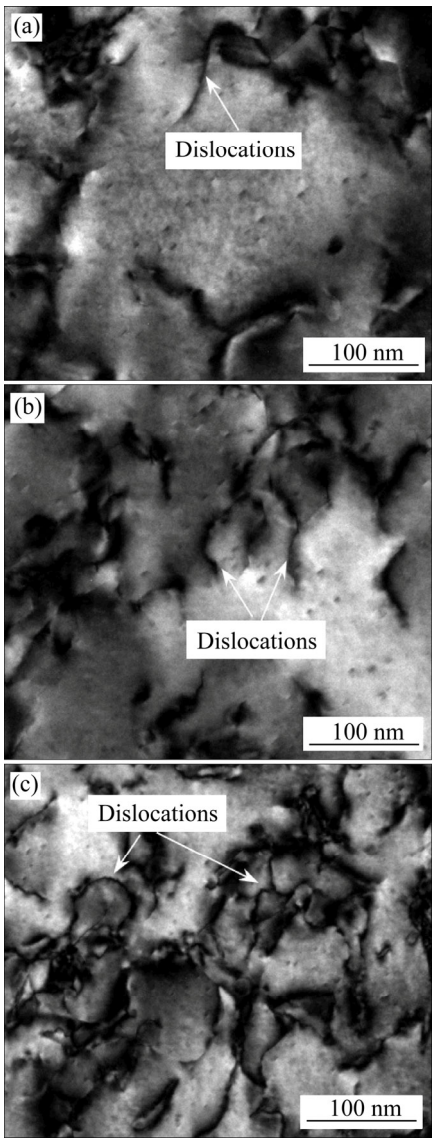

Figure 6 Bright field TEM images showing dislocations of samples aged at various temperatures for 1 h: (a) 155 °C; (b) 165 °C; (c) 175 °C

3.3.2 Distribution and size of T_1 precipitates

The HAADF-STEM images of the microstructures seen in the early creep aged samples at 155, 165 and 175 °C within 2 h are shown in Figure 7, taken along a $<110>_{Al}$ zone axis. After 2 h creep ageing at 155 °C, it is apparent from Figure 7(a) that a large fraction of β' precipitates, in the form of matrix. However, this effect of these β' precipitates formed at early natural ageing on the creep ageing

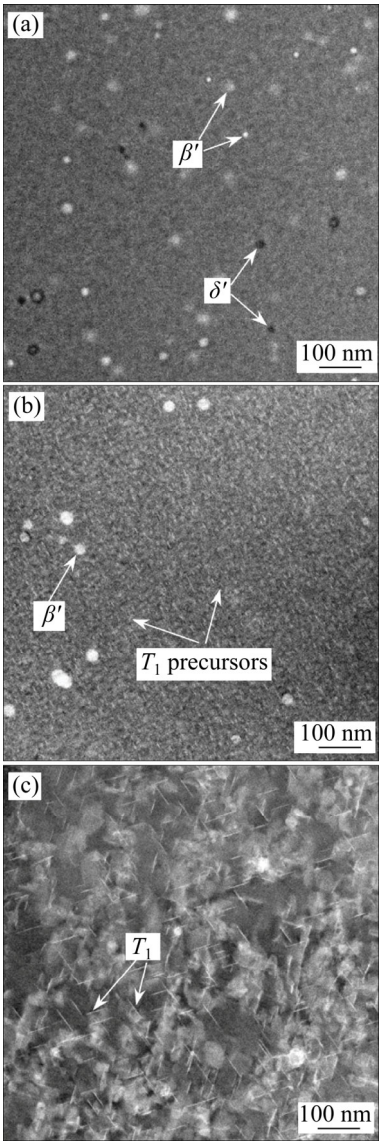

Figure 7 HAADF-STEM images of samples aged at different temperatures (close to <110>$_{Al}$ zone axis), showing microstructural evolution at early stage of creep ageing (within 2 h) under 180 MPa: (a) 155 °C; (b) 165 °C; (c) 175 °C

behaviour can be considered negligible, which attributes to the dissolution happening followed by further ageing at high temperatures [23]. Noted that no apparent T_1 precipitate was observed in the sample aged at 155 °C for 2 h. By contrast, the sample subjected to a higher temperature of 165 °C shows the presence of T_1 precipitates (designated as T_1 precursor here) with a high number fraction and very small dimension of within the Al matrix. Moreover, an obvious decrease in density of β' precipitates was observed, suggesting an occurrence of reversion at 165 °C for only 2 h. Qualitatively, Figure 7(c) shows a noteworthy growth in dimension of T_1 precipitates, at length and thickness directions, owing to further elevating ageing temperature to a higher level of 175 °C. In addition, some T_1 plates were also found to preferentially nucleate near some areas, where T_1 precipitation was relatively dense.

With increasing creep ageing time to 5 h, the sample aged at 155 °C was observed to have a certain number density and even smaller dimension of T_1 precipitates within the Al matrix, suggesting the formation of the T_1 precursors still goes on at this point. With further elevating temperature, it is apparent from Figure 8(b) that there is a significant white spherical particles, distributed in homogeneous dispersion state throughout the Al increase in the density and diameter of T_1 plates in the sample aged at 165 °C, compared to those aged

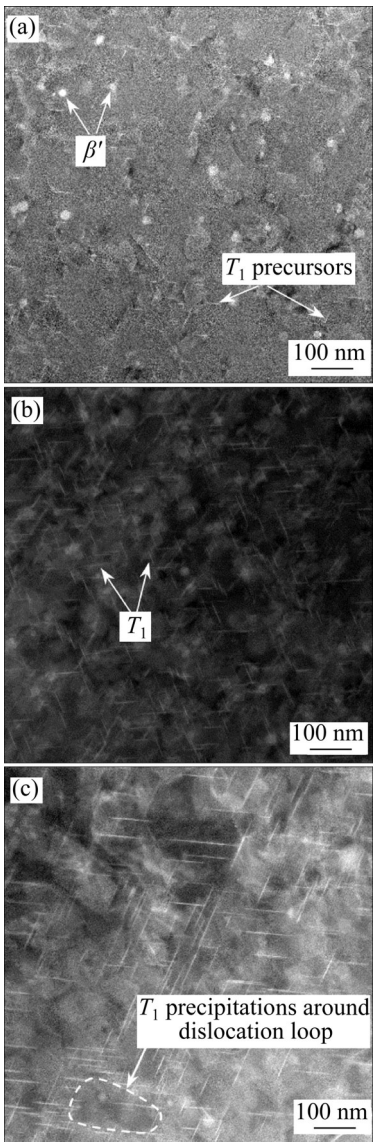

Figure 8 HAADF STEM images along <110>$_{Al}$ zone axis, of microstructure aged at different temperatures for 5 h: (a) 155 °C; (b) 165 °C; (c) 175 °C

at 155 °C. This indicates that the growth of T_1 precipitates plays a dominant role at this point for the sample aged at 165 °C. Comparing with the sample aged at 165 °C, there is an obvious increase in the T_1 plates diameter but almost little difference in number density (Figure 8(c)), by further raising temperature to 175 °C. Note that a special site of T_1 precipitation, in the form of the annulus, was observed to present in the sample subjected to higher temperature of 175 °C, which was potentially regarded as a dislocation loop attached with T_1 plates.

To further acquire information on the comparison of T_1 dimension obtained from samples aged at 155, 165 and 175 °C for 5 h, the size distributions of the T_1 plates (from at least 100 precipitates in several sample areas) were manually measured by Nano Measurer image processing software. The results in Figure 9 demonstrate that after creep ageing at 165 °C for 5 h the average precipitate diameter grows to 31.5 nm, which is much larger than that of the sample aged at 155 °C, 19.8 nm. The average T_1 plate diameter measured from the sample subjected to higher temperature of 175 °C further grows to 46.0 nm, which is more than twice that of the sample aged at 155 °C. This acceleration in T_1 precipitation by higher ageing temperatures is consistent with the observed changes in strength measured from specimens aged at different temperatures for the same ageing time.

From the microstructural results of the samples aged at 155, 165 and 175 °C in Section 3.3, this special "multi-stage creep feature" could be explained by an interaction mechanism between dislocations and diffusion, mainly including interactions between dislocations, dislocations and solid solutes, and precipitates. Schematic illustration in Figure 10(a) shows the microstructural evolution of the specimen aged at 155 °C during 180 MPa creep ageing tests. After the first 1 h of creep ageing test, dislocations introduced by creep deformation would be considered to reach a saturation status at this applied stress level of 180 MPa, which leads to the primary creep stage (Stage I) with a promptly decreasing creep strain rate. Simultaneously, segregation of solid solutes to the dislocations begins to happen during this period, preferentially in the regions in which the dislocations are most curved [16]. Compared to the end of Stage I, more significant segregation of solute atoms towards the

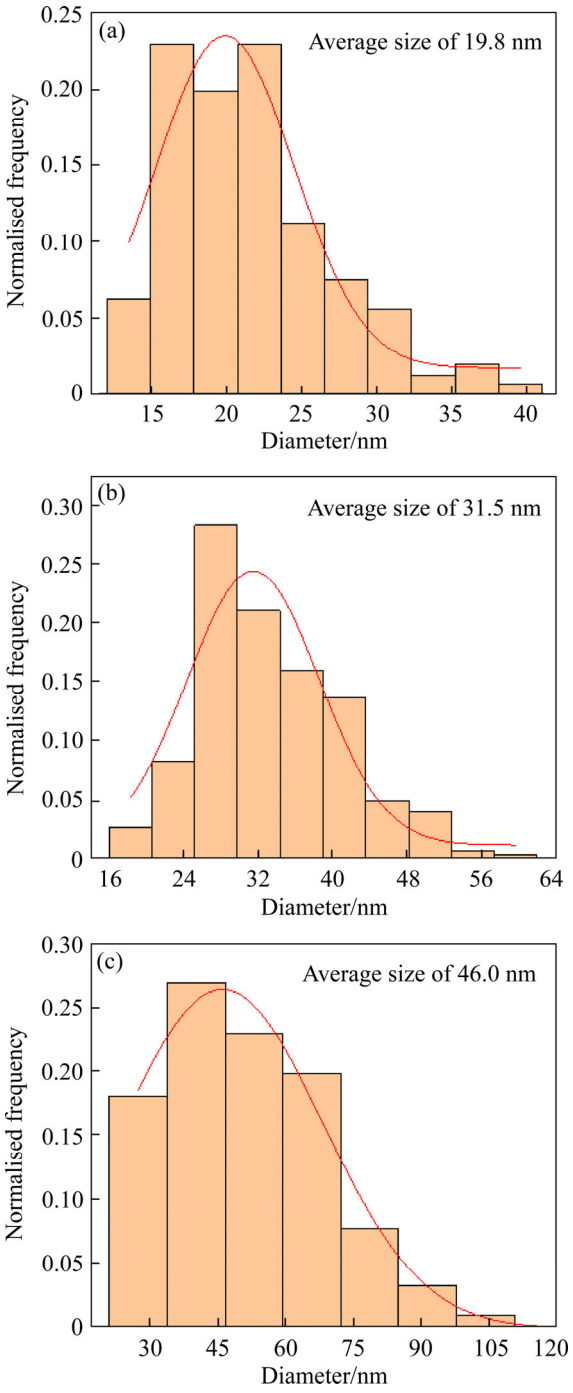

Figure 9 Average diameter and size distribution of T_1 plates in samples aged at different temperatures for 5 h measured from HAADF-STEM images: (a) 155 °C; (b) 165 °C; (c) 175 °C

dislocations could grow to solute atmospheres pinned dislocations, which is thought mainly responsible for Stage II with a creep strain rate of zero. During Stage III with an increasing creep strain rate, solute atoms would be fast depleted by the accelerated nucleation of T_1 precipitates around the dislocations, and further form the T_1 precursors,

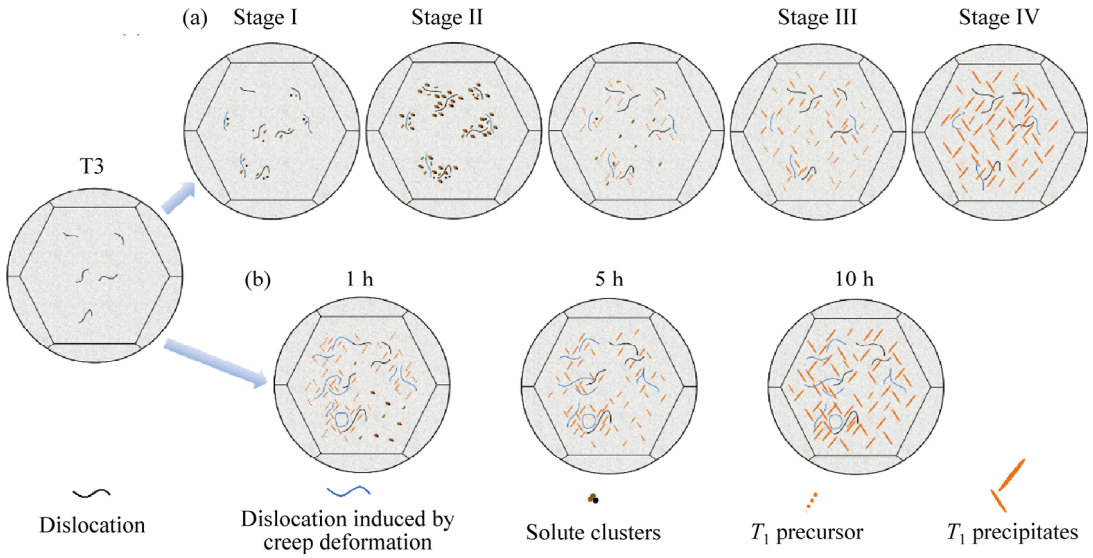

Figure 10 Schematic illustration of microstructure evolution during creep ageing tests aged at: (a) 155 °C; (b) 175 °C

which contributes to a decrease in the creep resistance of the materials. The microstructure, at the end of Stage III, consists of dislocations with T_1 precursors attached and a low density of small T_1 platelets nucleated at early stage (Stage II). This behaviour at Stage III can thus be attributed to the solute-depletion softening exceeding the age hardening effect of the T_1 precursors. Increasing creep ageing time to Stage IV, further growth of T_1 precipitates from its precursors would produce a stronger resistance to the motion of dislocations, which contributes to a decrease in creep rate to the relatively stable level, Stage IV of which determined by T_1 precipitation.

Moreover, a higher ageing temperature was found to result in a lower creep threshold stress under the same applied stress levels [18]. Namely, a higher density of dislocations could be introduced into the sample subjected to a higher temperature of 175 °C by creep deformation of 180 MPa, compared to that of the sample aged at 155 °C under the same stress. In line with observation of Section 3.3.1, dislocation density was clearly increasing when the temperature raised from 155 to 175 °C. As the solutes diffused towards the dislocations at Stage II, elevating the ageing temperatures increases the density of dislocations, resulting in a reduction of the average diffusion field size, so Stage II experiences a shorter timescale.

Schematic illustration in Figure 10(b) shows the microstructural evolutions of the sample subjected to 175 °C during 180 MPa creep ageing tests. Reaching a saturation level of dislocations by creep deformation was also considered as a main cause for a fast decreasing creep rate during the early creep ageing stage. Different kinds of dislocations can react with each other to give coalescing, rearrangement in thermal activation [24, 25]. Applying a higher temperature during creep ageing test can lead to an enhancement in interaction of dislocations, further resulting in the formation of larger dislocation structures by coalescence with each other, even including some tangled dislocation structures and dislocation loops. Meanwhile, an accelerated nucleation of T_1 precipitates occurs around the higher energy sites offered by the larger dislocation structures, which is attributed to an increasing diffusion of solute atoms at higher temperatures. Hence some T_1 plates preferentially precipitated on higher energy sites, such as dislocation loops, as observed in Figure 8(c). A balanced relation between the reduced mobility of these larger dislocation structures and solute-depletion softening is mostly responsible for a transient steady creep stage during the early creep ageing stage. After that, a slight decrease in creep strain rate until reaching a stable level would be dominant by the growth of T_1 precipitates, which provided a stronger resistance to the movement of dislocations.

Based on comparison of volume fraction and dimension of T_1 precipitates for the samples aged at 155, 165 and 175 °C at the same creep ageing time of 5 h, significantly higher strength is obtained in the specimen aged at 175 °C than that aged at 155 °C, which attributes to an acceleration in T_1 precipitation

by the higher temperatures. Further, this accelerated precipitation behaviour can be attributed to the combined effect of those larger dislocation structures and the enhanced diffusion of solid solutes, both induced by the higher temperature.

4 Conclusions

1) For the AA2198 alloy specimen subjected to 175 °C, the disappearance of Stage II and Stage III in the 155 °C creep curve and an increased creep strain, induced by the higher temperature, would significantly improve the efficiency of creep deformation during creep ageing tests. New insights into the multi-stage creep feature consisting of four creep stages are proposed for the AA2198 alloy. Stage I, Stage II and Stage III are controlled by interaction of dislocations and solid solutes, and Stage IV is controlled by the further growth of the T_1 precipitates.

2) The tensile test results indicate an acceleration in creep ageing to the peak-aged state by higher temperatures and almost the same peak strength and elongation for the specimens aged at 155, 165 and 175 °C.

3) Microstructure data from TEM observations reveal an increase in dislocation density with raising temperatures. Both larger dislocation lines and even tangled dislocation structures are observed in the sample aged at higher temperatures. This creep ageing behaviour at higher temperature of 175 °C can be attributed to the combined effects of the increased dislocation density, the formation of larger dislocation structures and enhanced diffusion of solid solutes, all by higher temperatures.

Contributors

The overarching research goals were developed by ZHAN Li-hua, ZHAO Xing and HUANG Ming-hui. ZHOU Chang and LI He provided the measured creep tests data, and analyzed the measured data. The initial draft of the manuscript was written by ZHOU Chang. All authors replied to the reviewers' comments and revised the final version.

Conflict of interest

ZHAN Li-hua, ZHOU Chang, LI He, ZHAO Xing, HUANG Ming-hui declare that they have no conflict of interest.

References

[1] JESHVAGHANI R A, EMAMI M, SHAHVERDI H R, HADAVI S M M. Effects of time and temperature on the creep forming of 7075 aluminum alloy: Springback and mechanical properties [J]. Materials Science and Engineering A, 2011, 528: 8795−8799. DOI: 10.1016/j.msea.2011.08.025.

[2] ZHAN Li-hua, LIN Jian-guo, DEAN T A. A review of the development of creep age forming: Experimentation, modelling and applications [J]. International Journal of Machine Tools and Manufacture, 2011, 51: 1−17. DOI: 10.1016/j.ijmachtools.2010.08.007.

[3] ZHAN Li-hua, LIN Jian-guo, DEAN T A, HUANG Ming-hui. Experimental studies and constitutive modelling of the hardening of aluminium alloy 7055 under creep age forming conditions [J]. International Journal of Mechanical Sciences, 2011, 53: 595−605. DOI: 10.1016/j.ijmecsci.2011.05.006.

[4] RIOJA R J, LIU J. The evolution of Al-Li base products for aerospace and space applications [J]. Metallurgical and Materials Transactions A, 2012, 43: 3325−3337. DOI: 10.1007/s11661-012-1155-z.

[5] WARNER T. Recently-developed aluminium solutions for aerospace applications [J]. Materials Science Forum, 2006, 519−521: 1271−1278. DOI: 10.4028/www.scientific.net/MSF.519-521.1271.

[6] KUMAR K S, BROWN S A, PICKENS J R. Microstructural evolution during aging of an Al-Cu-Li-Ag-Mg-Zr alloy [J]. Acta Materialia, 1996, 44: 1899−1915. DOI: 10.1016/1359-6454(95)00319-3.

[7] GAYLE F W, HEUBAUM F H, PICHENS J R. Structure and properties during aging of an ultra-high strength Al-Cu-Li-Ag-Mg alloy [J]. Scripta Metallurgica et Materialia, 1990, 24: 79−84. DOI: 10.1016/0956-716X(90)90570-7.

[8] NOBLE B, THOMPSON G E. T_1 (Al_2CuLi) precipitation in aluminium-copper-lithium alloys [J]. Metal Science Journal, 2013, 6: 167−174. DOI: 10.1179/030634572790445975.

[9] GANLE B M, ZHU A W, CSONTOS A A, STARKE E A Jr. The role of plastic deformation on the competitive microstructural evolution and mechanical properties of a novel Al-Li-Cu-X alloy [J]. Journal of Light Metals, 2001, 1: 1−14. DOI: 10.1016/S1471-5317(00)00002-X.

[10] DECREUS B, DESCHAMPS A, GEUSER F D, DONNADIEU P, SIGLI C, WEYLAND M. The influence of Cu/Li ratio on precipitation in Al-Cu-Li-X alloys [J]. Acta Materialia, 2013, 61: 2207−2218. DOI: 10.1016/j.actamat.2012.12.041.

[11] DONNADIEU P, SHAO Y, GEUSER F D, BOTTON G A, LAZAR S, CHEYNET M, BOISSIEU M D, DESCHAMPS A. Atomic structure of T_1 precipitates in Al-Li-Cu alloys revisited with HAADF-STEM imaging and small-angle X-ray scattering [J]. Acta Materialia, 2011, 59(2): 462−472. DOI: 10.1016/j.actamat.2010.09.044.

[12] NIE J F, MUDDLE B C. On the form of the age-hardening response in high strength aluminium alloys [J]. Materials Science and Engineering A, 2001, 319−321: 448−451. DOI: 10.1016/S0921-5093(01)01054-1.

[13] DESCHAMPS A, DECREUS B, GEUSER F D, DORIN T, WEYLANG M. The influence of precipitation on plastic deformation of Al–Cu–Li alloys [J]. Acta Materialia, 2013, 61: 4010−4021. DOI: 10.1016/j.actamat.2013.03.015.

[14] CSONTOS A A, STARKE E A. The effect of inhomogeneous plastic deformation on the ductility and fracture behavior of age hardenable aluminum alloys [J]. International Journal of Plasticity, 2005, 21(6): 1097−1118. DOI: 10.1016/j.ijplas.2004.03.003.

[15] RINGER S P, MUDDLE B C, POLMEAR I J. Effects of cold work on precipitation in Al-Cu-Mg-(Ag) and Al-Cu-Li-(Mg-Ag) alloys [J]. Metallurgical and Materials Transactions A, 1995, 26: 1659−1671. DOI: 10.1007/bf02670753.

[16] ARAULLO-PETERS V, GAULT B, GEUSER F D, DESCHAMPS A, CAIRNEY J M. Microstructural evolution during ageing of Al-Cu-Li-X alloys [J]. Acta Materialia, 2014, 66: 199−208. DOI: 10.1016/j.actamat.2013.12.001.

[17] DORIN T, GEUSER F D, LEFEBVRE W, SIGLI C, DESCHAMPS A. Strengthening mechanisms of T_1 precipitates and their influence on the plasticity of an Al-Cu-Li alloy [J]. Materials Science and Engineering A, 2014, 605: 119−126. DOI: 10.1016/j.msea.2014.03.024.

[18] LYU F, LI Yong, SHI Zhu-sheng, HUANG Xia, ZENG Yuan-song, LIN Jian-guo. Stress and temperature dependence of stress relaxation ageing behaviour of an Al-Zn-Mg alloy [J]. Materials Science and Engineering A, 2020, 773: 138859. DOI: 10.1016/j.msea.2019.138859.

[19] ZHANG Sai-fei, ZENG Wei-dong, YANG Wen-hua, SHI Chun-ling, WANG Hao-jun. Ageing response of a Al-Cu-Li 2198 alloy [J]. Materials and Design, 2014, 63: 368−374. DOI: 10.1016/j.matdes.2014.04.063.

[20] ZHU Xu-hao, LIN Y C, WU Qiang, JIANG Yu-qiang. Effects of aging on precipitation behavior and mechanical properties of a tensile deformed Al-Cu alloy [J]. Journal of Alloys and Compounds, 2020, 843: 155975. DOI: 10.1016/j.jallcom.2020.155975.

[21] ZOU Yan, CAO Ling-fei, WU Xiao-dong, WANG Yi-chang, SUN Xuan, SONG Hui, COUPER M J. Effect of ageing temperature on microstructure, mechanical property and corrosion behavior of aluminum alloy 7085 [J]. Journal of Alloys and Compounds, 2020, 823: 153792. DOI: 10.1016/j.jallcom.2020.153792.

[22] ZHOU Chang, ZHAN Li-hua, SHEN Ru-lin, ZHAO Xing, YU Hai-liang, HUANG Ming-hui, LI He, YANG You-liang, HU Li-bin, LIU De-bo, HU Zheng-gen. Creep behavior and mechanical properties of Al-Li-S4 alloy at different aging temperatures [J]. Journal of Central South University, 2020, 27(4): 1168−1175. DOI: 10.1007/s11771-020-4357-3.

[23] TSIVOULAS D, ROBSON J D. Heterogeneous Zr solute segregation and Al_3Zr dispersoid distributions in Al-Cu-Li alloys [J]. Acta Materialia, 2015, 93: 73−86. DOI: 10.1016/j.actamat.2015.03.057.

[24] LIU Chun-hui, MALLADI S K, XU Qiang, CHEN Jiang-hua, TICHELAAR F D, ZHUGE Xiao-dong, ZANDBERGEN H W. In-situ STEM imaging of growth and phase change of individual CuAlX precipitates in Al alloy [J]. Scientific Reports, 2017, 7: 2184. DOI: 10.1038/s41598-017-02081-9.

[25] ZHANG W, SUI M L, ZHOU Y Z, LI D X. Evolution of microstructures in materials induced by electropulsing [J]. Micron, 2003, 34(3−5): 189−198. DOI: 10.1016/S0968-4328(03)00025-8.

(Edited by FANG Jing-hua)

中文导读

温度对 Al-Cu-Li 合金在蠕变时效成形过程中蠕变行为、力学性能和微观组织的影响

摘要：在 180 MPa，20 h 的蠕变时效条件下，研究了 Al-Cu-Li 合金在 155~175 °C 的蠕变行为、微观组织和析出行为。温度的升高导致蠕变时效行为发生显著的变化，包括蠕变曲线的变化、蠕变时效早期蠕变速率的提高和蠕变量的增加。拉伸测试结果表明，在更高的温度下，试样提前达到峰值。利用透射电镜(TEM)观察温度对 AA2198 合金在蠕变时效成形中微观组织演化的影响。在更高温度时效的样品中观察到了更多较大的位错，甚至有缠结的位错结构。在相同的时间内，温度越高，T_1 相析出的越多。根据分析结果建立了一种新的机制，解释了温度对微观结构演化和蠕变行为的影响。该机制考虑了由更高温度引起的更大的位错结构的形成和溶质原子向这些更大的或缠结的位错扩散的综合效应。

关键词：Al-Cu-Li 合金；蠕变时效成形；力学性能；微观组织；析出行为